

**ESTIMATING THE PROBABILITY DISTRIBUTIONS OF  
ALLOY IMPACT TOUGHNESS: A CONSTRAINED  
QUANTILE REGRESSION APPROACH**

ALEXANDR GOLODNIKOV

*Department of Industrial and Systems Engineering  
University of Florida, Gainesville, FL 32611, USA*

YEVGENY MACHERET

*Institute for Defense Analysis  
Alexandria, VA 22311, USA*

A ALEXANDRE TRINDADE

*Department of Statistics  
University of Florida, Gainesville, FL 32611, USA*

STAN URYASEV\*, GRIGORIY ZRAZHEVSKY

*Department of Industrial and Systems Engineering  
University of Florida, Gainesville, FL 32611, USA*

We extend our earlier work, Golodnikov *et al* [3] and Golodnikov *et al* [4], by estimating the entire probability distributions for the impact toughness characteristic of steels, as measured by Charpy V-Notch (CVN) at  $-84^{\circ}\text{C}$ . Quantile regression, constrained to produce monotone quantile function and unimodal density function estimates, is used to construct the empirical quantiles as a function of various alloy chemical composition and processing variables. The estimated quantiles are used to produce an estimate of the underlying probability density function, rendered in the form of a histogram. The resulting CVN distributions are much more informative for alloy design than singular test data. Using the distributions to make decisions for selecting better alloys should lead to a more effective and comprehensive approach than the one based on the minimum value from a multiple of the three test, as is commonly practiced in the industry.

---

\*corresponding author. e-mail: uryasev@ufl.edu

## 1. Introduction

In recent work, Golodnikov *et al* [3] developed statistical models to predict the tensile yield strength and toughness behavior of high strength low alloy (HSLA-100) steel. The yield strength was shown to be well approximated by a linear regression model. The alloy toughness (as evaluated by a Charpy V-notch, CVN, at  $-84^{\circ}\text{C}$  test), was modeled by fitting separate quantile regressions to the 20th, 50th, and 80th percentiles of its probability distributions. The toughness model was shown to be reasonably accurate. Ranking of the alloys and selection of the best composition and processing parameters based on the strength and toughness regression models, produced similar results to the experimental alloy development program.

Models with the capability to estimate the effect of processing parameters and chemical composition on toughness, are particularly important for alloy design. While the tensile strength can be modeled with reasonable accuracy by, for example, Neural Networks (Metzbower and Czyryca [10]), the prediction of CVN values remains a difficult problem. One of the reasons for this is that experimental CVN data often exhibit substantial scatter. The Charpy test does not provide a measure of an invariant material property, and CVN values depend on many parameters, including specimen geometry, stress distribution around the notch, and microstructural inhomogeneities around the notch tip. More on the CVN test, including the reasons behind the scatter and statistical aspects of this type of data analysis, can be found in McClintock and Argon [9], Corowin and Houghland [2], Lucon *et al* [8], and Todinov [13].

Developing alloys with minimum allowable CVN values, therefore, results in multiple specimens for each experimental condition, leading to complex and expensive experimental programs. In addition, it is possible that optimum combinations of processing parameters and alloy compositions will be missed due to the practical limitations on the number of experimental alloys and processing conditions. This issue was addressed by Golodnikov *et al* [4], in a follow-up paper to Golodnikov *et al* [3]. The statistical models developed therein, could be used to simulate a multitude of experimental conditions with the objective of identifying better alloys on the strength vs. toughness diagram, and determining the chemical composition and processing parameters of the optimal alloys. The optimization was formulated as a linear programming problem with constraints. The solution (the efficient frontier) plotted on the strength-toughness diagram, could be used as an aid in successively refining the experimental program, directing the

characteristics of the resulting alloys ever closer to the efficient frontier.

The objective of this paper is to build on our previous two papers, by estimating the entire distribution function of CVN at  $-84^\circ\text{C}$  values for all specimens of steel analyzed in Golodnikov *et al* [3], and for selected specimens on the efficient frontiers considered by Golodnikov *et al* [4]. As a tool we use quantile regression, simultaneously fitting a model to several percentiles, while constraining the solution in order to obtain sensible estimates for the underlying distributions. To this end, Section 2 outlines the details and reasoning behind the methodology to be used. The methodology is applied to the steel dataset in Section 3.

## 2. Estimating the Quantile Function With Constrained Quantile Regression

For a random variable  $Y$  with distribution function  $F_Y(y) = P(Y \leq y)$  and  $0 \leq \theta \leq 1$ , the  $\theta$ th quantile function of  $Y$ ,  $Q_Y(\theta)$ , is defined to be

$$Q_Y(\theta) = F_Y^{-1}(y) = \inf\{y \mid F_Y(y) \geq \theta\}.$$

For a random sample  $Y_1, \dots, Y_n$  with empirical distribution function  $\hat{F}_Y(y)$ , we define the  $\theta$ th empirical quantile function as

$$\hat{Q}_Y(\theta) = \hat{F}_Y^{-1}(y) = \inf\{y \mid \hat{F}_Y(y) \geq \theta\},$$

which can be determined by solving the minimization problem

$$\hat{Q}_Y(\theta) = \arg \min_y \left\{ \sum_{i \mid Y_i \geq y} \theta |Y_i - y| + \sum_{i \mid Y_i \leq y} (1 - \theta) |Y_i - y| \right\}.$$

Introduced by Koenker and Bassett [5], the  $\theta$ th **quantile regression** function is a generalization of the  $\theta$ th quantile function to the case when  $Y$  is a linear function of a vector of  $k + 1$  explanatory variables  $\mathbf{x}' = [1, x_1, \dots, x_k]$  plus random error,  $Y = \mathbf{x}'\boldsymbol{\beta} + \varepsilon$ . Here,  $\boldsymbol{\beta}' = [\beta_0, \beta_1, \dots, \beta_k]$  are the regression coefficients, and  $\varepsilon$  is a random variable that accounts for the surplus variability or scatter in  $Y$  that cannot be explained by  $\mathbf{x}$ . The  $\theta$ th quantile function of  $Y$  can therefore be written as

$$Q_Y(\theta|\mathbf{x}) = \inf\{y \mid F_Y(y|\mathbf{x}) \geq \theta\} \equiv \mathbf{x}'\boldsymbol{\beta}(\theta), \tag{1}$$

where  $\boldsymbol{\beta}(\theta)' = [\beta_0(\theta), \beta_1(\theta), \dots, \beta_k(\theta)]$ . The relationship between the ordinary regression and the quantile regression coefficients,  $\boldsymbol{\beta}$  and  $\boldsymbol{\beta}(\theta)$ , is in general not a straightforward one. Given a sample of observations  $y_1, \dots, y_n$  from  $Y$ , with corresponding observed values  $\mathbf{x}_1, \dots, \mathbf{x}_n$  for the explanatory

306 A. Golodnikov, Y. Macheret, A. Trindade, S. Uryasev and G. Zrazhevsky

variables, estimates of the quantile regression coefficients can be obtained as follows:

$$\hat{\beta}(\theta) = \arg \min_{\beta(\theta) \in \mathcal{R}^{k+1}} \left\{ \sum_{i|y_i \geq \mathbf{x}'_i \beta(\theta)} \theta |y_i - \mathbf{x}'_i \beta(\theta)| + \sum_{i|y_i \leq \mathbf{x}'_i \beta(\theta)} (1 - \theta) |y_i - \mathbf{x}'_i \beta(\theta)| \right\}. \quad (2)$$

This minimization can be reduced to a linear programming problem and solved via standard optimization methods. A detailed discussion of the underlying optimization theory and methods is provided by Portnoy and Koenker [11]. The value  $\hat{Q}_Y(\theta|\mathbf{x}) = \mathbf{x}'\hat{\beta}(\theta)$  is then the estimated  $\theta$ th quantile (or  $100\theta$ th percentile) of the response variable  $Y$  at  $\mathbf{x}$  (instead of the estimated mean value of  $Y$  at  $\mathbf{x}$  as would be the case in ordinary – least squares – regression).

Instead of restricting attention to a single quantile,  $\theta$ , one can in fact solve (2) for all  $\theta \in [0, 1]$ , and thus recover the entire conditional quantile function (equivalently, the conditional distribution function) of  $Y$ . Efficient algorithms for accomplishing this have been proposed by Koenker and d'Orey [7], who show that this results in  $H_n$  distinct quantile regression hyperplanes, with  $\mathbf{E}(H_n) = O(n \log n)$ . Although Bassett and Koenker [6] show that the estimated conditional quantile function at the mean value of  $\mathbf{x}$  is a monotone jump function on the interval  $[0, 1]$ , for a general design point the quantile hyperplanes are not guaranteed to be parallel, and thus  $\hat{Q}_Y(\theta|\mathbf{x})$  may not be a proper quantile function. This also usually results in multimodal estimated probability density functions, which may not be desirable in certain applications.

In order to ensure proper and unimodal estimated distributions are obtained from the quantile regression optimization problem, we introduce additional constraints in (2), and simultaneously estimate  $\beta(\theta_j)$ ,  $j = 1, \dots, m$ , over a grid of probabilities,  $0 < \theta_1 < \dots < \theta_m < 1$ . That is, with  $Q(\theta_j|\mathbf{x}_i) = \mathbf{x}'_i \beta(\theta_j)$  denoting the  $\theta_j$ th quantile function of  $Y$  at  $\mathbf{x}_i$ , we solve the following expression for the  $((k + 1) \times m)$  matrix whose  $j$ th column is  $\beta(\theta_j)$ :

$$\arg \min_{\beta(\theta_j) \in \mathcal{R}^{k+1}, j=1, \dots, m} \sum_{i=1}^n \sum_{j=1}^m \left\{ (1 - \theta_j) [Q(\theta_j|\mathbf{x}_i) - y_i]^+ + \theta_j [y_i - Q(\theta_j|\mathbf{x}_i)]^+ \right\}, \quad (3)$$

where for a real number  $z$ ,  $(z)^+$  denotes the positive part of  $z$  (equal to  $z$  itself if it is positive, zero otherwise). The following additional constraints are imposed on (3).

- **Monotonicity.** This is obtained by requiring that quantile hyperplanes corresponding to larger probabilities be larger than those corresponding to smaller ones, i.e.

$$Q(\theta_{j+1}|\mathbf{x}_i) \geq Q(\theta_j|\mathbf{x}_i), \quad j = 1, \dots, m-1, \quad i = 1, \dots, n. \quad (4)$$

- **Unimodality.** Suppose the conditional probability density of  $Y$ ,  $f_Y(\cdot|\mathbf{x})$ , is unimodal with mode occurring at the quantile  $\theta^*$ . Let  $\theta_{m_1} < \theta^* < \theta_{m_2}$ , for some indices  $m_1 < m_2$  in the chosen grid. Then, the probability density is monotonically increasing over quantiles  $\{\theta_1, \dots, \theta_{m_1}\}$ , and monotonically decreasing over quantiles  $\{\theta_{m_2}, \dots, \theta_m\}$ . Over  $\{\theta_{m_1}, \dots, \theta_{m_2}\}$ , the probability density first increases monotonically up to  $\theta^*$ , then decreases monotonically. The following expressions, to be satisfied for all  $i = 1, \dots, n$ , formalize these (approximately) sufficient conditions for unimodality:

$$Q(\theta_{j+2}|\mathbf{x}_i) - 2Q(\theta_{j+1}|\mathbf{x}_i) + Q(\theta_j|\mathbf{x}_i) < 0, \quad j = 1, \dots, m_1 - 2, \quad (5)$$

$$Q(\theta_{j+3}|\mathbf{x}_i) - 3Q(\theta_{j+2}|\mathbf{x}_i) + 3Q(\theta_{j+1}|\mathbf{x}_i) - Q(\theta_j|\mathbf{x}_i) > 0, \quad (6)$$

$$j = m_1, \dots, m_2 - 3,$$

$$Q(\theta_{j+2}|\mathbf{x}_i) - 2Q(\theta_{j+1}|\mathbf{x}_i) + Q(\theta_j|\mathbf{x}_i) > 0, \quad j = m_2, \dots, m - 2. \quad (7)$$

Requiring monotonicity leads immediately to (4). Substantiation of (5)-(7) as sufficient conditions for unimodality (in the limit as  $m \rightarrow \infty$ ) is not so straightforward, and is deferred to Appendix A. We summarize these requirements formally as an estimation problem.

**Estimation Problem** (Unimodal Conditional Probability Density). *Conditional quantile estimates of  $Y$  based on in-sample data  $y_1, \dots, y_n$  and  $\mathbf{x}_1, \dots, \mathbf{x}_n$ , can be obtained by solving (3) over the grid  $0 < \theta_1 < \dots < \theta_m < 1$ , subject to constraints (4) and (5)-(7). The resulting  $\theta$ th quantile estimate at any given in-sample design point  $\mathbf{x}_i$ ,  $\hat{Q}(\theta|\mathbf{x}_i) = \mathbf{x}_i' \hat{\beta}(\theta)$ , is by construction monotone in  $\theta$  for  $\theta \in \{\theta_1, \dots, \theta_m\}$ . Constraints (5)-(7) are approximate sufficient conditions for unimodality of the associated density.*

Estimation Problem 1 can be solved in two steps. First omit the unimodality constraints by solving (3) subject only to (4). Analyzing the sample of  $m$  empirical quantile estimates thus obtained, determine indices  $m_1$  and  $m_2$  that define a probable quantile interval,  $\theta_{m_1} < \hat{\theta}^* < \theta_{m_2}$ , around

308 A. Golodnikov, Y. Macheret, A. Trindade, S. Uryasev and G. Zrazhevsky

the mode of the empirical density function,  $\hat{\theta}^*$ . In the second step the full problem (3)-(7) is solved.

Although the literature on nonparametric unimodal density estimation is vast (see for example Cheng *et al* [1]), we are not aware of any work that approaches the problem from the quantile regression perspective, as we have proposed it. In fact, we are not proposing a method for density estimation *per se*, rather quantile construction with a view toward imparting desirable properties on the associated density. As far as we are able to ascertain, Taylor and Bunn [12] is in fact the only paper to date dealing with constrained quantile regression, albeit in the context of combining forecast quantiles for data observed over time. Focusing on the effects of imposing constraints on the quantile regression problem, they conclude that this leads in general to a loss in the unbiasedness property for the resulting estimates.

### 3. Case Study: Estimating the Impact Toughness Distribution of Steel Alloys

In Golodnikov *et al* [3], we developed statistical regression models to predict tensile yield strength (Yield), and fracture toughness (as measured by Charpy V-Notch, CVN, at  $-84^\circ\text{C}$ ) of High Strength Low Alloy (HSLA-100) steel. These predictions are based on a particular steel's chemical composition, namely C ( $x_1$ ), Mn ( $x_2$ ), Si ( $x_3$ ), Cr ( $x_4$ ), Ni ( $x_5$ ), Mo ( $x_6$ ), Cu ( $x_7$ ), Cb ( $x_8$ ), Al ( $x_9$ ), N ( $x_{10}$ ), P ( $x_{11}$ ), S ( $x_{12}$ ), V ( $x_{13}$ ), measured in weight percent, and the three alloy processing parameters: plate thickness in mm (Thick,  $x_{16}$ ), solution treating (Aust,  $x_{14}$ ), and aging temperature (Aging,  $x_{15}$ ). As described in the analysis of Golodnikov *et al* [3], the yield strength, chemical composition, and temperature data, have been normalized by their average values.

Finding that the CVN data had too much scatter to be usefully modeled via ordinary regression models, Golodnikov *et al* [3] instead fitted separate quantile regression models, each targeting a specific percentile of the CVN distribution. In particular, the 20%th percentile of the distribution function of CVN is of interest in this analysis, since it plausibly models the smallest of the three values of CVN associated with each specimen (which is used as the minimum acceptability threshold for a specimen's CVN value). Letting  $\hat{Q}(0.2)$  denote the estimated 20th percentile of the conditional distribution

function of log CVN, the following model was obtained:

$$\hat{Q}(0.2) = 0.000 - 0.1x_2 + 0.04x_4 - 0.419x_6 + 0.608x_7 - 0.144x_{10} \\ - 0.035x_{13} - 0.693x_{14} + 1.692x_{15} - 0.004x_{16}. \quad (8)$$

(CVN was modeled on the logarithmic scale in order to guarantee that model-predicted values would always be positive.) Although not quite as successful as the model for Yield, the  $R^1(0.2) = 52\%$  value and further goodness of fit analyses showed this model to be sufficiently useful for its intended purpose, the selection and ranking of good candidate steels (Golodnikov *et al* [3]).

Using the method described in Section 2, we now seek to extend (8) by estimating the CVN conditional quantiles functions for several quantiles simultaneously, and for all specimens of steels described in Golodnikov *et al* [3] and some points on the efficient frontier determined by Golodnikov *et al* [4]. This dataset had an overall sample size of  $n = 234$ . We used a grid of  $m = 99$  quantiles,  $\{\theta_j = j/100\}$ ,  $j = 1, \dots, 99$ . The resulting histograms estimate the conditional densities, and are presented in Appendix B. Each histogram is based on the 99 values,  $\{\hat{Q}(0.01), \dots, \hat{Q}(0.99)\}$ .

We discuss three of these histograms, that illustrate distinct types of behavior of interest in metallurgy. The three dots appearing in each histogram identify the location of the observed values of CVN at  $-84^\circ C^a$ . The most decisive cases are those where the entire probability density falls either above or below the minimum acceptability threshold of 2.568 for CVN (0.943 on the log scale). The histogram on Figure 2 corresponding to steel #16, is an example of the former, while the first histogram of Figure 5 (steel #28 with Thick= 51, Aust= 1.05 and Aging= 0.84) is an example of the latter case. The first histogram of Figure 1 (steel #1) illustrates the intermediate case, less desirable from a metallurgy perspective, since a positive probability for CVN values to straddle the minimum acceptability threshold leads to greater uncertainty in the screening of acceptable specimens.

#### 4. Summary

We extended our earlier work, Golodnikov *et al* [3] and Golodnikov *et al* [4], by estimating the entire probability distributions for the impact toughness

<sup>a</sup>If less than three dots are displayed, then two or more CVN values coincide.

310 A. Golodnikov, Y. Macheret, A. Trindade, S. Uryasev and G. Zrazhevsky

characteristic of steels, as measured by Charpy V-Notch at  $-84^{\circ}\text{C}$ . Quantile regression, constrained to produce monotone quantile function and unimodal density function estimates, was used to construct empirical quantiles which were subsequently rendered in the form of a histogram. The resulting CVN distributions are much more informative for alloy design than singular test data. Using the distributions to make decisions for selecting better alloys should lead to a more effective and comprehensive approach than the one based on the minimum value from a multiple of the three test, as is commonly practiced in the industry. These distributions may be also used as a basis for subsequent reliability and risk modeling.

## References

1. M. Cheng, T. Gasser and P. Hall (1999). "Nonparametric density estimation under unimodality and monotonicity constraints", *Journal of Computational and Graphical Statistics*, 8, 1-21.
2. W.R. Corwin and A.M. Houghland, (1986). "Effect of specimen size and material condition on the Charpy impact properties of 9Cr-1Mo-V-Nb steel", in: *The Use of Small-Scale Specimens for Testing Irradiated Material*, ASTM STP 888, (Philadelphia, PA) 325-338.
3. A. Golodnikov, Y. Macheret, A. Trindade, S. Uryasev and G. Zrazhevsky, (2005). "Modeling Composition and Processing Parameters for the Development of Steel Alloys: A Statistical Approach", *Research Report # 2005-1*, Department of Industrial and Systems Engineering, University of Florida.
4. A. Golodnikov, Y. Macheret, A. Trindade, S. Uryasev and G. Zrazhevsky, (2005). "Optimization of Composition and Processing Parameters for the Development of Steel Alloys: A Statistical Approach", *Research Report # 2005-2*, Department of Industrial and Systems Engineering, University of Florida.
5. R. Koenker and G. Bassett (1978). "Regression Quantiles", *Econometrica*, 46, 33-50.
6. G. Bassett and R. Koenker (1982). "An empirical quantile function for linear models with iid errors", *Journal of the American Statistical Association*, 77, 407-415.
7. R. Koenker, and V. d'Orey (1987; 1994). "Computing regression quantiles", *Applied Statistics*, 36, 383-393; and 43, 410-414.
8. E. Lucon *et al*(1999). "Characterizing Material Properties by the Use of Full-Size and Sub-Size Charpy Tests", in: *Pendulum Impact Testing: A Century of Progress*, ASTM STP 1380, T. Siewert and M.P. Manahan, Sr. eds., American Society for Testing and Materials, (West Conshohocken, PA) 146-163.
9. F.A. McClintock and A.S. Argon (1966). *Mechanical Behavior of Materials*, (Reading, Massachusetts), Addison-Wesley Publishing Company, Inc.
10. E.A. Metzbower and E.J. Czyryca (2002). "Neural Network Analysis of HSLA Steels", in: T.S. Srivatsan, D.R. Lesuer, and E.M. Taleff eds., *Modeling the*



*Performance of Engineering Structural Materials*, TMS.

11. S. Portnoy and R. Koenker (1997). “The Gaussian hare and the Laplacian tortoise: Computability of squared-error versus absolute-error estimators”, *Statistical Science*, 12, 279-300.
12. J.W. Taylor and D.W. Bunn (1998). “Combining forecast quantiles using quantile regression: Investigating the derived weights, estimator bias and imposing constraints”, *Journal of Applied Statistics*, 25, 193-206.
13. M.T. Todinov (2004). “Uncertainty and risk associated with the Charpy impact energy of multi-run welds”, *Nuclear Engineering and Design*, 231, 27-38.

### Appendix A. Substantiation of the Unimodality Constraints

Let  $F(x) = P(X \leq x)$  and  $f(x) = F'(x)$  be respectively, the cumulative distribution function (cdf), and probability density function (pdf), for random variable  $X$ , and assume the cdf to be continuously differentiable on  $\mathbf{R}$ . Suppose  $f(x) > 0$  over the open interval  $(x_l, x_r)$ , whose endpoints are quantiles corresponding to probabilities  $\theta_l = F(x_l)$  and  $\theta_r = F(x_r)$ . Then for  $\theta \in (\theta_l, \theta_r)$ , the quantile function of  $X$  is uniquely defined as the inverse of the cdf,  $Q(\theta) \equiv F^{-1}(\theta) = x$ . Now, differentiating both sides of the identity  $F(Q(\theta)) = \theta$ , we obtain for  $x \in (x_l, x_r)$ ,

$$f(x) = \frac{1}{dQ/d\theta} \Big|_{\theta=F(x)}. \tag{A.1}$$

This implies that since  $f(x) > 0$  on  $(x_l, x_r)$ ,  $dQ/d\theta > 0$ , and therefore  $Q(\theta)$  is monotonically increasing on  $(\theta_l, \theta_r)$ . Differentiating (A.1) once more gives

$$f'(x) = -\frac{d^2Q/d\theta^2}{(dQ/d\theta)^2} \Big|_{\theta=F(x)}. \tag{A.2}$$

With the above in mind, we can now state our main result.

**Proposition 1** *If  $Q(\theta)$  is three times differentiable on  $(\theta_l, \theta_r)$  with  $d^3Q/d\theta^3 > 0$ , then  $f(x)$  is unimodal (has at most one extremum) on  $[x_l, x_r]$ .*

**Proof:** Since  $d^3Q/d\theta^3 > 0$ , it follows that  $d^2Q/d\theta^2$  is continuous and monotonically increasing on  $(\theta_l, \theta_r)$ . Therefore,  $d^2Q/d\theta^2|_{\theta_l} < d^2Q/d\theta^2|_{\theta_r}$ , and there are 3 cases to consider:

- (i)  $d^2Q/d\theta^2|_{\theta_l} < d^2Q/d\theta^2|_{\theta_r} < 0$ . Recalling that  $dQ/d\theta > 0$  for all  $\theta \in (\theta_l, \theta_r)$ , it follows from (A.2) that  $f'(x) > 0$ . Therefore  $f(x)$  is monotonically increasing and has no extrema on  $(x_l, x_r)$ . Consequently, the maximum value of  $f(x)$  on  $[x_l, x_r]$  is attained at  $x = x_r$ .

312 A. Golodnikov, Y. Macheret, A. Trindade, S. Uryasev and G. Zrazhevsky

- (ii) There exists a  $\theta^* \in (\theta_l, \theta_r)$  such that  $d^2Q/d\theta^2 < 0$  on  $(\theta_l, \theta^*)$ , and  $d^2Q/d\theta^2 > 0$  on  $(\theta^*, \theta_r)$ . Then  $f'(x) > 0$  on  $[x_l, x^*)$ , and  $f'(x) < 0$  on  $(x^*, x_r]$ . Therefore,  $f(x)$  has exactly one extremum on  $[x_l, x_r]$ , a maximum occurring at  $x^* = Q(\theta^*)$ .
- (iii)  $0 < d^2Q/d\theta^2|_{\theta_l} < d^2Q/d\theta^2|_{\theta_r}$ . As in case (i), but the numerator of (A.2) is now positive, which implies  $f'(x) < 0$ . Therefore  $f(x)$  is monotonically decreasing and has no extrema on  $(x_l, x_r)$ . Consequently, the maximum value of  $f(x)$  on  $[x_l, x_r]$  is attained at  $x = x_l$ . □

The three unimodality constraints (5)-(7), are the discretized empirical formulation of the three cases in this proof. To see this, let  $\delta = 1/(m + 1)$  be the inter-quantile grid point distance, and  $Q(\theta)$  denote the conditional quantile function of  $Y$ , where for notational simplicity we suppress the dependence of  $Q(\cdot)$  on the  $x_i$ . We then have that for large  $m$ ,

$$\begin{aligned} \left. \frac{dQ(\theta)}{d\theta} \right|_{\theta_j} &\approx \frac{Q(\theta_{j+1}) - Q(\theta_j)}{\delta} \\ \left. \frac{d^2Q(\theta)}{d\theta^2} \right|_{\theta_j} &\approx \frac{Q'(\theta_{j+1}) - Q'(\theta_j)}{\delta} \approx \frac{Q(\theta_{j+2}) - 2Q(\theta_{j+1}) + Q(\theta_j)}{\delta^2} \end{aligned} \tag{A.3}$$

$$\begin{aligned} \left. \frac{d^3Q(\theta)}{d\theta^3} \right|_{\theta_j} &\approx \frac{Q''(\theta_{j+1}) - Q''(\theta_j)}{\delta} \approx \\ &\approx \frac{Q(\theta_{j+3}) - 3Q(\theta_{j+2}) + 3Q(\theta_{j+1}) - Q(\theta_j)}{\delta^3}. \end{aligned} \tag{A.4}$$

Now, recall for example that the pdf of  $Y$  is required to be monotonically increasing over quantiles  $\{\theta_1, \dots, \theta_{m_1}\}$ . Since this corresponds to case (i) in the Proposition, from (A.3) a sufficient condition (in the limit as  $m \rightarrow \infty$ ) is that  $Q(\theta_{j+2}) - 2Q(\theta_{j+1}) + Q(\theta_j) < 0$ , for all  $j = 1, \dots, m_1$ . Similarly, the pdf of  $Y$  is required to be monotonically decreasing over  $\{\theta_{m_2}, \dots, \theta_m\}$  which corresponds to case (iii), and can be obtained by having  $Q(\theta_{j+2}) - 2Q(\theta_{j+1}) + Q(\theta_j) > 0$ , for all  $j = m_2, \dots, m$ . Finally, over  $\{\theta_{m_1}, \dots, \theta_{m_2}\}$  the pdf of  $Y$  has at most one mode. From the statement of the Proposition, this is ensured if  $Q(\theta_j)$  has a positive 3rd derivative, which from (A.4) corresponds to  $Q(\theta_{j+3}) - 3Q(\theta_{j+2}) + 3Q(\theta_{j+1}) - Q(\theta_j) > 0$ , for all  $j = m_1, \dots, m_2$ .

**Appendix B. Histograms for Selected Distributions of log CVN at  $-84^{\circ}\text{C}$**

Figure 1. Estimated distribution of log CVN at  $-84^{\circ}\text{C}$  for Steels #1-12. The location of each of the three observed CVN values is indicated with a dot.

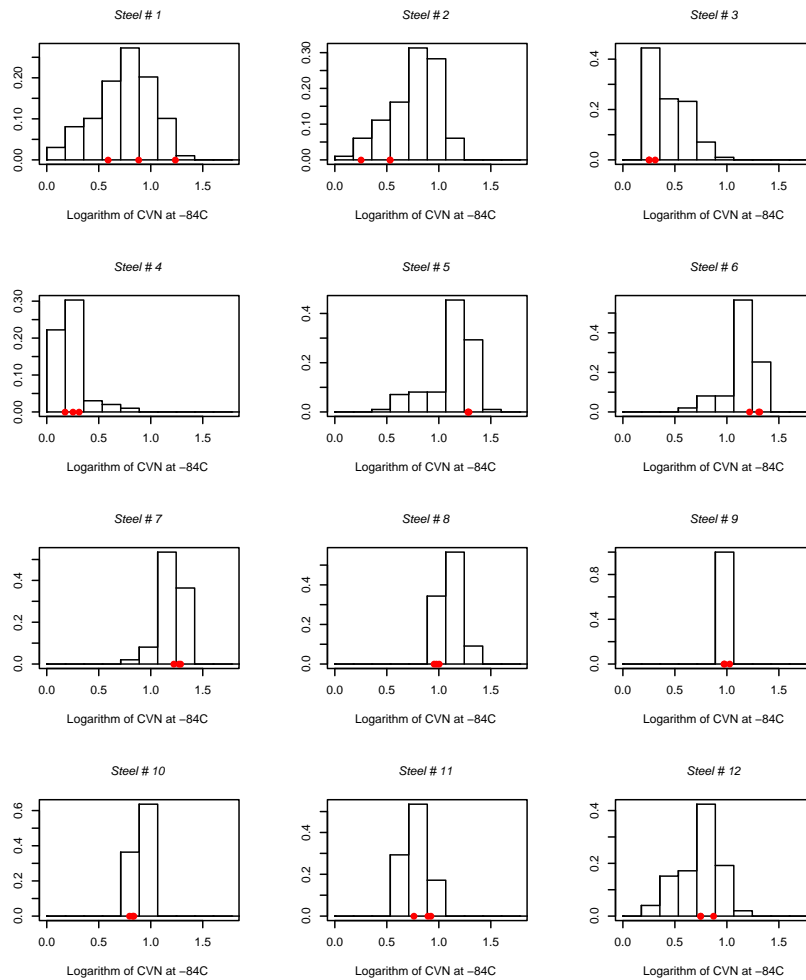
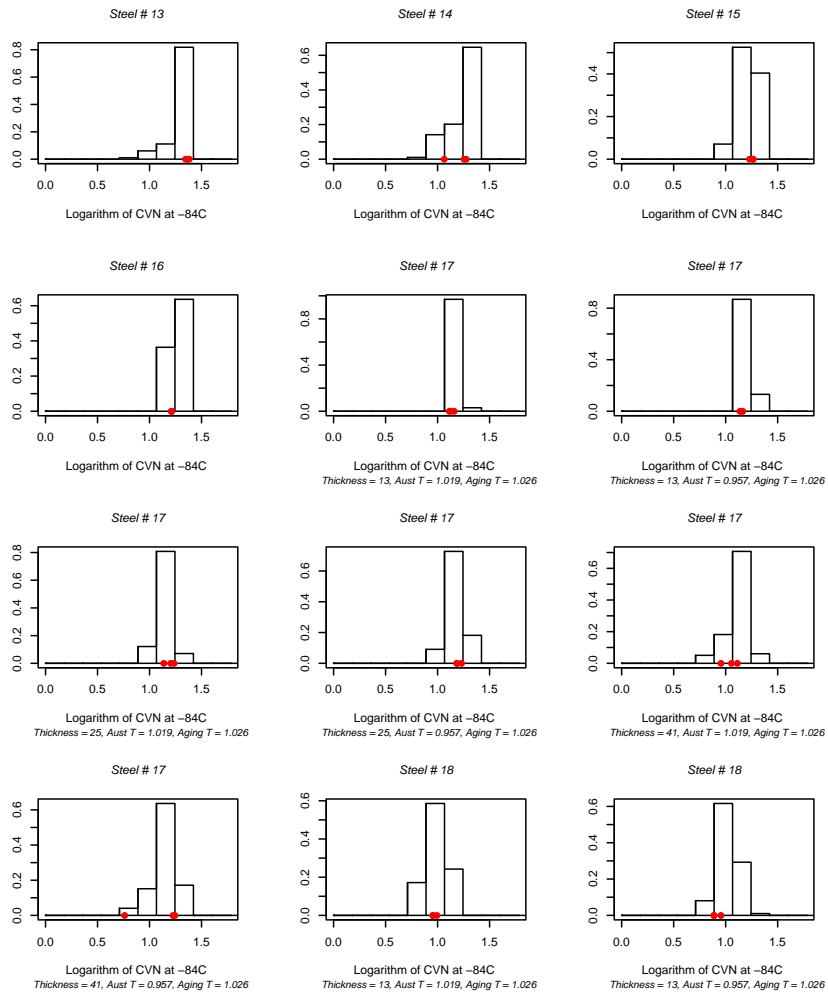


Figure 2. Estimated distribution of log CVN at  $-84^{\circ}\text{C}$  for Steels #13-18. The location of each of the three observed CVN values is indicated with a dot.



*Estimating the Probability Distributions of Alloy Impact Toughness* 315

Figure 3. Estimated distribution of log CVN at  $-84^{\circ}\text{C}$  for Steels #18 (continued) and #24. The location of each of the three observed CVN values is indicated with a dot.

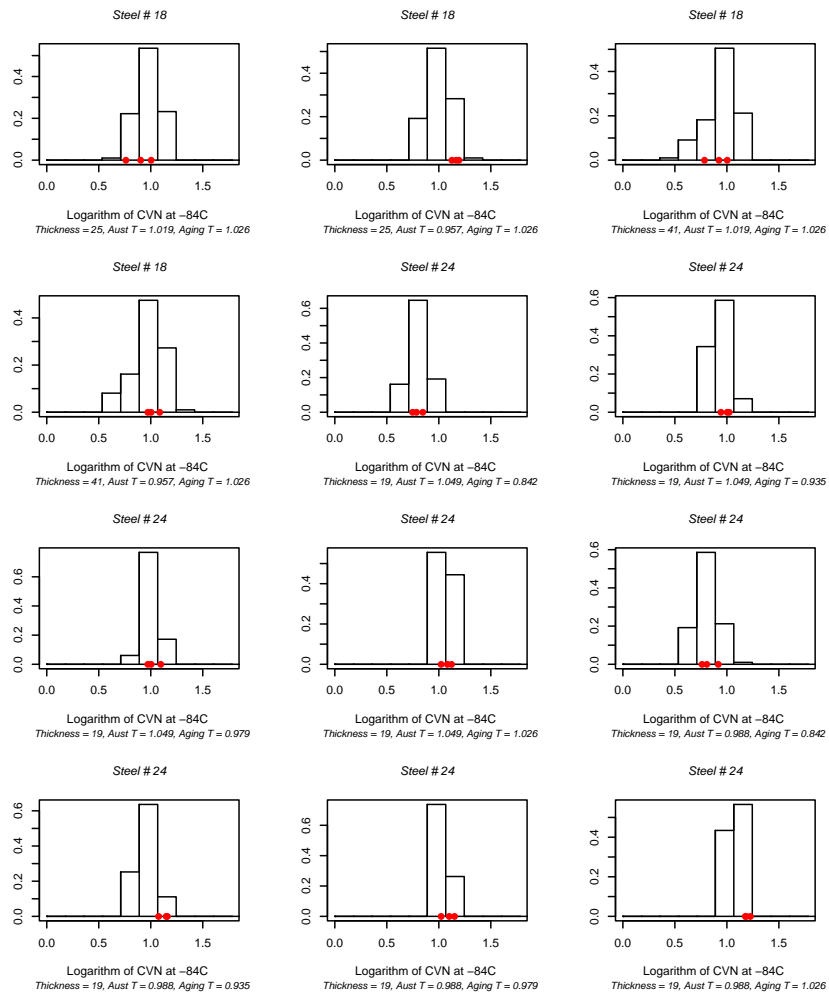
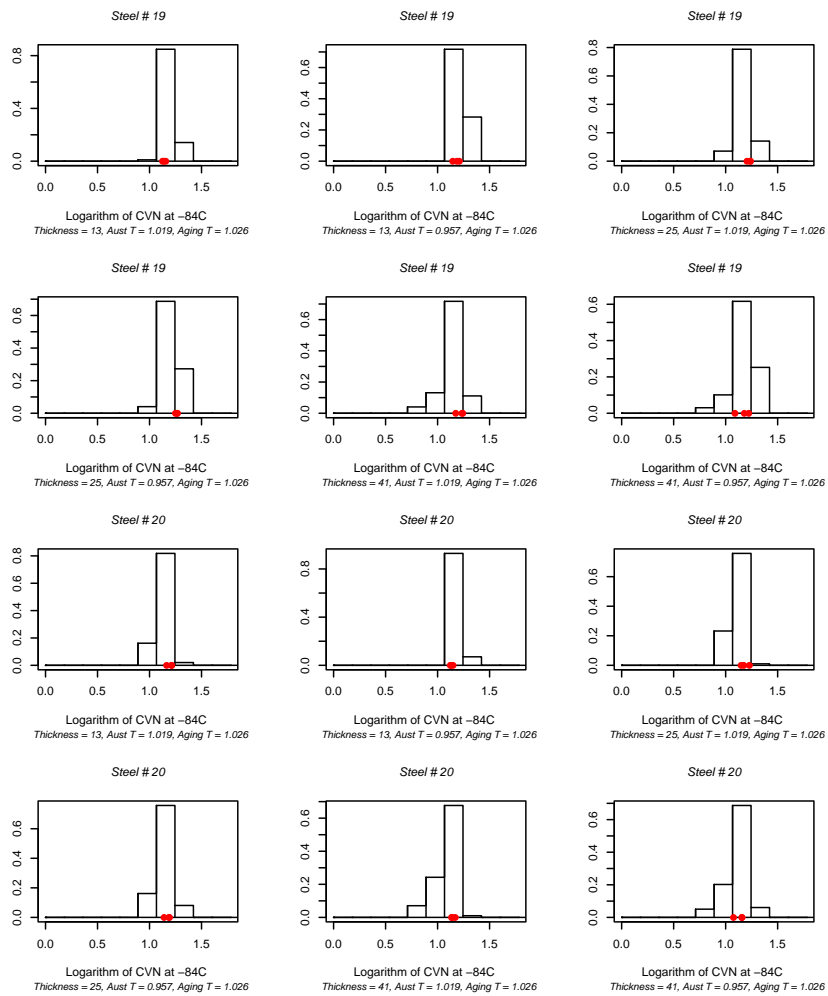


Figure 4. Estimated distribution of log CVN at  $-84^{\circ}\text{C}$  for Steels #19-20. The location of each of the three observed CVN values is indicated with a dot.



*Estimating the Probability Distributions of Alloy Impact Toughness 317*

Figure 5. Estimated distribution of log CVN at  $-84^{\circ}\text{C}$  for Steel #28. The location of each of the three observed CVN values is indicated with a dot.

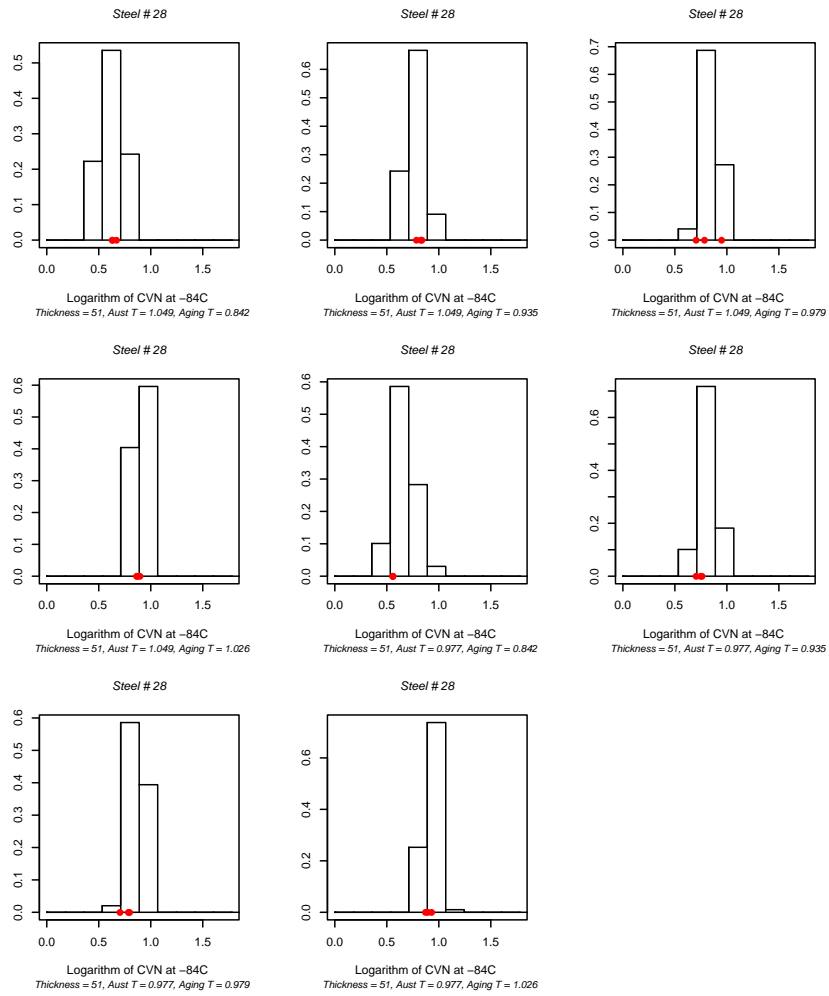


Figure 6. Estimated distribution of log CVN at  $-84^{\circ}\text{C}$  for 6 points on the efficient frontier.

